*Korean J. Chem. Eng.*, **30**(3), 649-657 (2013)
DOI: 10.1007/s11814-012-0169-y

# Response surface methodology approach to optimize coagulation-flocculation process using composite coagulants

**Tiroyaone Tshukudu*, Huaili Zheng*,†, Xuebin Hua*, Jun Yang*, Mingzhuo Tan**, Jiangya Ma*, Yongjun Sun*, and Guocheng Zhu***

*Key Laboratory of the Three Gorges Reservoir Regions Eco-Environment, Ministry of Education, Chongqing University, Chongqing 400045, China
**Jiangmen Wealth Water Purifying Agent Co., Ltd., Jiangmen City, Guangdong 529000, China
(*Received 13 May 2012 • accepted 2 October 2012*)

**Abstract**−Response surface method and experimental design were applied as alternatives to the conventional methods for optimization of the coagulation test. A central composite design was used to build models for predicting and optimizing the coagulation process. The model equations were derived using the least square method of the Minitab 16 software. In these equations, the removal efficiency of turbidity and COD were expressed as second-order functions of the coagulant dosage and coagulation pH. By applying RSM, the optimum condition using $PFPD_1$ was coagulant dosage of 384 mg/L and coagulation pH of 7.75. The optimum condition using $PFPD_2$ was coagulant dosage of 390 mg/L and coagulation pH of 7.48. Confirmation experiment demonstrated a good agreement between experimental values and model predicted. This demonstrates that RSM and CCD can be successfully applied for modeling and optimizing the coagulation process using $PFPD_1$ and $PFPD_2$.

Key words: Analysis of Variance (ANOVA), Optimizing, Central Composite Design (CCD), Turbidity Removal, COD Removal

## INTRODUCTION

Municipal wastewater is a combination of different types of wastewaters originating from the sanitary system of commercial housing, industrial facilities and institutions, in addition to any groundwater, surface and storm water that may be present. Because of economic development, increasing volumes of wastewater generated daily contain various chemical substances and solid particles, which are a serious threat to human health. The ultimate goal of wastewater management is the protection of the environment with public health and socio-economic concerns. A very important step in water/wastewater treatment is the coagulation-flocculation process that is used because of its simplicity and cost effectiveness. Regardless of the nature of the treated sample and the overall treatment scheme, coagulation-flocculation either is usually included as a pre-, or post-treatment step [1-3]. The application of coagulation-flocculation combined with other appropriate physicochemical or biological treatment processes such as ozonation, photo-oxidation, or submerged biological filters, results in enhanced efficiency during wastewater treatment [4]. However, the process largely depends on the role of coagulants-flocculants. Therefore, there is a need for improving the treatment efficiency during the coagulation-flocculation process to solve this problem [2,3]. Many factors, such as the amount of particulate material, natural organic matter (NOM) present and the chemical/physical properties affect the performance of coagulation. However, the conditions of coagulation, such as coagulant type, dose, and pH affect the coagulation-flocculation process [5,6].

The key issue with experimental design is the selection of experimental strategies in parameter design. The two most important characteristics in determining the choice of experimental design are strength of interactions between variables and the degree of pure experimental error. Generally, the most frequently used methods of design of experiment (DOE) are the partial or full factorial design, response surface methodology (RSM) and the Taguchi approach. However, coagulation-flocculation optimization practices in many studies are performed on a trial and error basis using the conventional one-factor-at-a-time (OFAT) method. The method consists of selecting a starting point, or baseline set of levels, for each factor, and then successfully varying each factor over its range with the other factors held constant at the baseline level. After the tests are performed, a series of plots are constructed showing how the response variable was affected by varying each factor with all other factors held constant [7,8]. This single dimension search is laborious, time consuming, and incapable of reaching the true optimum due to neglecting the interactions among variables [5,6,9-12]. In recent years, several types of statistical experimental design methods have been employed to overcome these limitations [13]. RSM has been proposed to determine the influence of individual factors and the influence of their interactions. It was initially developed for determining optimum operating conditions in the chemical industry, but is now used in a variety of fields and applications [5,13,14]. RSM, initially developed and described by Box and Wilson, is a collection of statistical methods for modelling problems where several independent variables (inputs) influence a dependent response variable (output) with an explicit objective of optimizing this response even in the presence of complex interaction [13]. Several studies have reported the examination of the coagulation-flocculation pro-

†To whom correspondence should be addressed.
E-mail: zhl@cqu.edu.cn, ZHL6512@126.com

cess for the treatment of industrial wastewater, especially with respect to performance optimization of coagulant/flocculant, determination of experimental conditions, assessment of pH and investigation of flocculant dosage [12]. In addition, removal of turbidity and chemical oxygen demand (COD) by coagulation/flocculation method is a well-researched topic; however, in this study, RSM was used to analyze the data.

Composite coagulants have been extensively studied and applied to water treatment systems today because of their superior efficiency compared with traditional inorganic coagulants, and lower cost compared with organic coagulants [15]. Nowadays, a new method of using composite coagulants, in which an inorganic coagulant is premixed with an organic coagulant before the coagulant is used to treat water, has been applied in many investigations. In this study, Poly-Ferric-Sulfate (PFS) and PolyDiAllylDiMethylAmmonium (PDADMAC) composite coagulants, $PFPD_1$ (96.5% PFS and 3.5% PDADMAC) and $PFPD_2$ (89.5% PFS and 10.5% PDADMAC) were investigated. The investigation aims at optimization of the coagulant dosage and coagulation pH to achieve highest removal of turbidity and COD from wastewater using the composite coagulants, $PFPF_1$ and $PFPD_2$. The optimization is carried out via central composite design (CCD) and RSM experimental design. The interaction between factors influencing turbidity and COD removal is established and models describing the effect of the factors on turbidity and COD removal efficiency are also described.

## MATERIAL AND METHODS

### 1. Materials

All reagents used in this study were analytical grade except diallydimethyl ammonium chloride (DADMAC) and PFS, which were technical grade. The other reagents used were 2,2′-Azobis[2-(2-imidazolin-2-yl)propane] dihydrochloride ($V_{a044}$), sodium hydroxide (NaOH), and hydrochloric acid (HCl). All aqueous solutions and standard solutions were prepared with de-ionized water. The wastewater was collected from the sewer system of Chongqing University. After filtering to remove large particles, the samples were used for coagulation-flocculation experiments immediately.

### 2. Preparation of Composite Coagulant

PDADMAC used in this experiment was a product prepared in the laboratory. First, 20 g of DADMAC monomer was added to a reaction vessel, followed by 0.15 g of $V_{a044}$ as the initiator to prepare the monomer phase. Then, 10 mL of de-ionized water used to rinse the glassware after transferring the monomer and initiator to the reaction vessel was added to the mixture. The mixture was purged using nitrogen gas with agitation to remove oxygen for 20 min; lastly, the reaction vessel was heated with a thermostatic controlled water to 50 ºC, which was maintained for 8 h. The resulting polymer solution was cooled to room temperature before storage.

The composite coagulants were prepared by taking a measured amount of PDADMAC (3.5% and 10.5%) and then mixing it with PFS solution. The mixture was stirred thoroughly with a magnetic stirrer until it was absolutely mixed to prepare composite coagulants $PFPD_1$, and $PFPD_2$.

### 3. Characterization of Composite Coagulant

Samples of PFS, $PFPD_1$ and $PFPD_2$ were dried at 55 ºC in an oven for several days. They were then mixed with potassium bromide (KBr) to prepare a pellet, suitable for Fourier transformed infra red (FT-IR) spectrophotometer analysis. An FT-IR spectrum was

**Table 1. Experimental ranges and significant levels of factors**

| Factors | Ranges and levels | | | | |
|---|---|---|---|---|---|
| | −2 | −1 | 0 | 1 | 2 |
| $PFDP_1$ dosage (mg/L) | 310 | 350 | 390 | 430 | 470 |
| $PFPD_2$ dosage (mg/L) | 310 | 350 | 390 | 430 | 470 |
| pH | 6.5 | 7.0 | 7.5 | 8.0 | 8.5 |

**Table 2. Experimental design and results obtained for turbidity and COD removal efficiency**

| Run | Experimental design | | Results | | | | | | | |
|---|---|---|---|---|---|---|---|---|---|---|
| | | | $PFPD_1$ | | | | $PFPD_2$ | | | |
| | | | Turbidity removal | | COD removal | | Turbidity removal | | COD removal | |
| | Dosage | pH | Exp. | Pred. | Exp. | Pred. | Exp. | Pred. | Exp. | Pred. |
| 1 | 350 | 8 | 96.86 | 96.73 | 66.49 | 65.97 | 87.64 | 87.93 | 59.33 | 60.95 |
| 2 | 390 | 6.5 | 95.40 | 95.60 | 60.31 | 59.11 | 88.59 | 88.11 | 55.50 | 55.17 |
| 3 | 430 | 7 | 97.13 | 96.96 | 62.89 | 64.76 | 90.97 | 91.41 | 57.89 | 57.92 |
| 4 | 390 | 7.5 | 97.66 | 97.95 | 67.53 | 65.61 | 91.76 | 90.50 | 69.38 | 67.61 |
| 5 | 350 | 7 | 97.80 | 97.43 | 57.22 | 58.41 | 86.05 | 86.92 | 63.64 | 65.10 |
| 6 | 390 | 8.5 | 96.05 | 96.00 | 61.34 | 61.86 | 86.69 | 86.79 | 57.89 | 57.40 |
| 7 | 470 | 7.5 | 97.93 | 97.91 | 58.25 | 57.57 | 89.70 | 89.73 | 54.55 | 54.85 |
| 8 | 390 | 7.5 | 98.31 | 97.95 | 64.95 | 65.61 | 90.17 | 90.50 | 68.42 | 67.61 |
| 9 | 390 | 7.5 | 98.11 | 97.95 | 64.43 | 65.61 | 90.97 | 90.50 | 66.51 | 67.61 |
| 10 | 310 | 7.5 | 96.87 | 97.05 | 57.22 | 57.22 | 84.47 | 84.07 | 59.81 | 58.68 |
| 11 | 390 | 7.5 | 97.64 | 97.95 | 65.98 | 65.61 | 90.33 | 90.50 | 67.94 | 67.61 |
| 12 | 390 | 7.5 | 97.70 | 97.95 | 66.49 | 65.61 | 90.02 | 90.50 | 67.46 | 67.61 |
| 13 | 430 | 8 | 98.00 | 98.06 | 59.79 | 59.95 | 89.22 | 89.09 | 64.11 | 64.30 |

Exp. is the measured removal efficiency; Pred. is the predicted removal efficiency recorded in the range of 4,000-400 $cm^{-1}$. In addition, a scanning electron microscope (SEM) examined the surface morphology of the coagulants.

**4. Coagulation-flocculation Experiments**

The coagulation-flocculation experiments were carried out using a program-controlled jar test apparatus (ZR4-6, Zhongrun Water Industry Technology Development Co. Ltd., China) at room temperature. 500 ml of wastewater was transferred into a beaker, and the initial pH was adjusted to the set value using 0.5 M HCl and NaOH. Under rapid mixing with the set agitation speed of 300 rpm, predetermined amount of coagulant was dosed. After 2 min, the speed was changed to a slow speed of 50 rpm for 10 min; lastly, after quiescent settling of 120 min, the clarified wastewater was extracted from 2 cm below the surface for measurement of residual turbidity and COD. The turbidity of the supernatant was measured with a turbidity-meter (HACH 2100p, HACH Company, USA) while COD was measured with a HACH COD reactor.

**5. Response Surface Methodology (RSM)**

The Minitab-16 software was used for statistical design of experiments and data analysis. In this study, CCD and RSM were applied to optimize coagulant dosage and coagulation pH. To define the experimental domain explored, preliminary experiments were carried out to determine a narrower, more effective range of coagulant dose and pH prior to designing the experimental runs. The coagulant dosage and coagulation pH ranges selected for investigation are given in Table 1. Table 2 shows the experimental design and results obtained for turbidity and COD removal.

The response variable can be expressed as a function of the independent process variables according to the following response surface quadratic model [13,14]:

$$Y = \beta_o + \sum_{i=1}^{k}\beta_i x_i + \sum_{i=1}^{k}\beta_{ii} x_i^2 + \sum_{i=1}\sum_{j=i+1}\beta_{ij} x_i x_j + \varepsilon \qquad (1)$$

where Y is the predicted response; $x_i$ and $x_j$ are the factors that influence the predicted response Y; $\beta_i$, $\beta_{ij}$ and $\beta_{ij}$ are the coefficient of linear, interaction and quadratic terms, respectively; k the number of factors studied and optimized in the experiment and $\varepsilon$ is the random error.

The regression analysis for the quadratic equation model was determined using the Minitab-16 software. First, the feasibility of the quadratic equation model between the test and response variables was established using analysis of variance (ANOVA). Then, F-test and P-values (probability) with 95% confidence level were used to check for the statistical significance of the quadratic equation model and test variables. Second, in order to test the model fit, the modeling quality of the model was determined using the coefficient of determination ($R^2$). The scientific software Origin version 8.0 software was used for response surface plots.

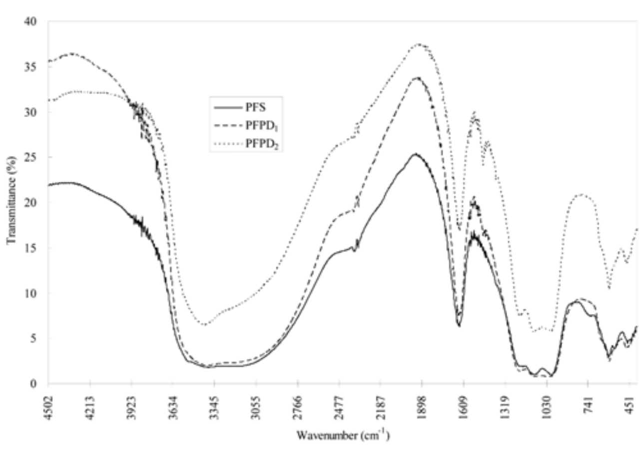


**Fig. 1. FTIR spectral analysis of PFS, PFPD$_1$ and PFPD$_2$.**

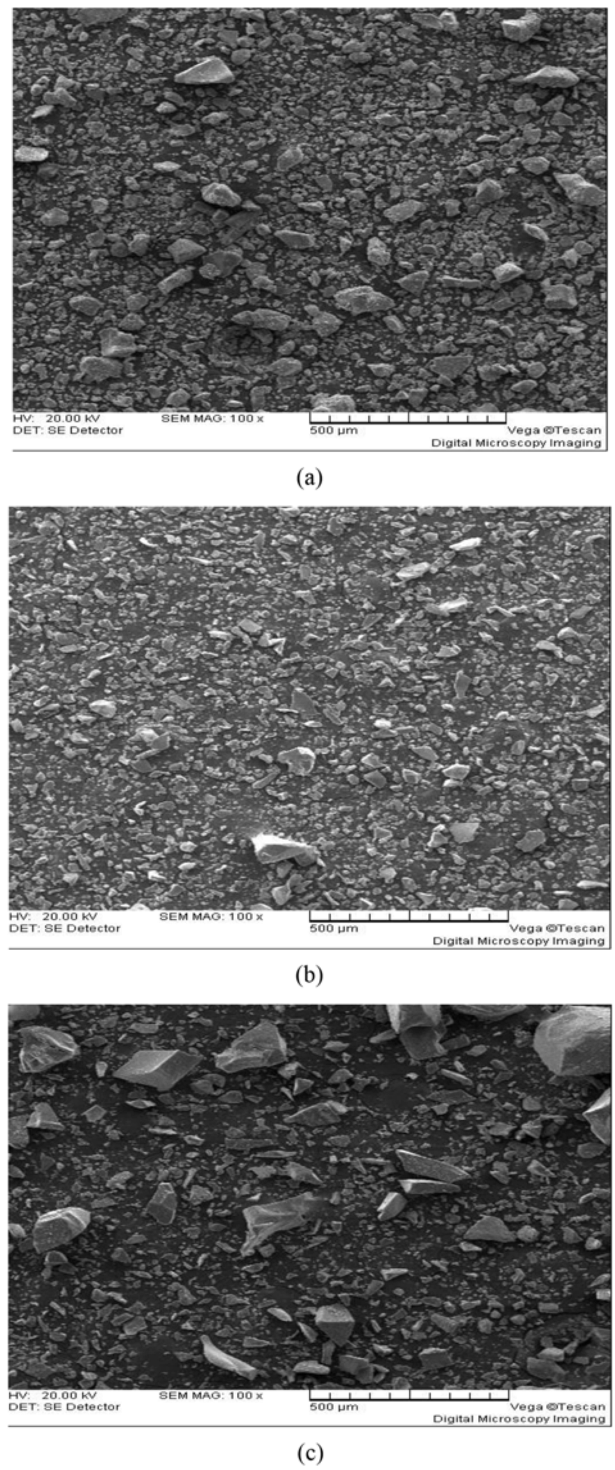


**Fig. 2. SEM photographs for (a) PFS, (b) PFPD$_1$ and (c) PFPD$_2$.**

## RESULTS AND DISCUSSION

### 1. Characterization of Coagulants

FT-IR and SEM instruments were used to analyze and characterize the structure and morphology of the coagulants.

1-1. FTIR Spectra Analysis

The possible chemical bonds in PFS, $PFPD_1$ and $PFPD_2$ were investigated by examining the FT-IR characteristic peaks in the range 4,000-400 $cm^{-1}$ with KBr as dispersant for matching the corresponding chemical bonds. Fig. 1 shows the FT-IR spectrum for PFS, $PFPD_1$ and $PFPD_2$.

The figure shows that the spectrum of PFS is similar to $PFPD_1$ and $PFPD_2$ except for the extra peak at around 1,470 $cm^{-1}$ in the spectra of $PFPD_1$ and $PFPD_2$. Compared with the structure of PDADMAC, the peak at 1,470 $cm^{-1}$ in the spectra of $PFPD_1$ and $PFPD_2$ is the characteristic absorption peak for PDADMAC. Therefore, overlapping the spectrum indicates the spectra of $PFPD_1$ and $PFPD_2$ are similar to the combination of the PFS and PDADMAC spectra. This indicates that no new chemical bond was created when PFS was mixed with PDADMAC, which means that $PFPD_1$ and $PFPD_2$ were physical mixtures. The finding of Gao et al. [16] that by mixing Poly-Ferric Chloride (PFC) and PDADMAC, no new chemical bond was created supports this.

1-2. SEM Images

The surface morphologies of PFS, $PFPD_1$ and $PFPD_2$ were analyzed using a SEM.

Fig. 2 shows the surface morphology of PFS, $PFPD_1$ and $PFPD_2$. It shows PFS, $PFPD_1$ and $PFPD_2$ as irregular surfaces randomly forming aggregates of various sizes and shapes. Apart from the irregular surface, a compact solid structure was observed. Zeng and Park [17] reported that compact net structures are more favorable to coagulate colloidal particles and form bridge-aggregation among flocs when compared with the branched structure [17,18].

### 2. Model Fitting

The purpose of this experiment was to use the experimental data to compute the model using the least square method. Therefore, the two responses (turbidity and COD removal efficiency) were correlated with the two factors (coagulant dosage and coagulation pH) using the second order polynomial according to Eq. (1). From the experimental data (Table 2), the following quadratic regression models were obtained for turbidity and COD removal efficiency.

$$Y_{Turb1}=28.5217-0.1070X_1+23.5929X_2-0.0001X_1^2-2.1457X_2^2+0.0226X_1X_2 \quad (2)$$
$(R^2=92.57\%, \text{adj. } R^2=87.26\%)$

$$Y_{COD1}=-880.969+2.163X_1+138.47X_2-0.001X_1^2-5.119X_2^2-0.155X_1X_2 \quad (3)$$
$(R^2=91.69\%, \text{adj. } R^2=85.75\%)$

$$Y_{Turb2}=-297.073+0.786X_1+61.284X_2-0.001X_1^2-3.048X_2^2-0.043X_1X_2 \quad (4)$$
$(R^2=93.60\%, \text{adj. } R^2=89.03\%)$

$$Y_{COD2}=-441.489+0.311X_1+119.698X_2-0.002X_1^2-11.327X_2^2+0.132X_1X_2 \quad (5)$$
$(R^2=96.45\%, \text{adj. } R^2=93.92\%)$

Eqs. (2) and (3) are the quadratic regression models for turbidity and COD removal using $PFPD_1$, while Eqs. (4) and (5) are the quadratic regression models for turbidity and COD removal using $PFPD_2$. $X_1$ and $X_2$ are the coagulant dosage and coagulation pH, respectively.

### 3. Validation of the Model

Graphical and numerical methods were used to validate the models in this study. The statistical testing of the model was performed using Fisher's statistical test for ANOVA. Table 3 shows the ANOVA result for turbidity and COD removal efficiencies. The P-value is used to judge whether F-statistics is large enough to indicate statistical significance. A P-value lower than 0.05 indicates that the model is considered to be statistically significant [5,6,19]. Therefore, Table 3 demonstrates the quadratic regression models of turbidity and COD removal using $PFPD_1$ were statistically significant at the 5% confi-

**Table 3. ANOVA results for response parameters**

| | Turbidity removal | | | | COD removal | | | |
|---|---|---|---|---|---|---|---|---|
| | Sum of square | Mean square | F-value | P-value | Sum of square | Mean square | F-value | P-value |
| $PFPD_1$ | | | | | | | | |
| Regression | 8.1296 | 1.6259 | 17.43 | 0.001 | 152.694 | 30.539 | 15.44 | 0.001 |
| Linear | 0.69 | 2.9303 | 31.42 | 0.000 | 5.757 | 55.360 | 28.00 | 0.000 |
| Square | 6.6256 | 3.3128 | 35.52 | 0.002 | 108.68 | 54.338 | 27.48 | 0.000 |
| Interactions | 0.8140 | 0.8140 | 8.73 | 0.021 | 38.261 | 38.261 | 19.35 | 0.003 |
| Total error | 0.6528 | 0.0933 | 13.841 | 1.977 | | | | |
| Lack of fit | 0.2803 | 0.0935 | 1.00 | 0.478 | 7.783 | 2.594 | 1.71 | 0.302 |
| Pure error | 0.3725 | 0.09312 | 6.058 | 1.515 | | | | |
| $PFPD_2$ | | | | | | | | |
| Regression | 53.014 | 10.6029 | 20.49 | 0.000 | 316.881 | 63.376 | 38.07 | 0.000 |
| Linear | 25.270 | 8.6577 | 16.73 | 0.002 | 14.728 | 38.317 | 23.01 | 0.001 |
| Square | 24.975 | 12.4875 | 24.13 | 0.001 | 274.452 | 137.226 | 82.42 | 0.000 |
| Interactions | 2.769 | 2.769 | 5.35 | 0.054 | 27.701 | 27.701 | 16.64 | 0.005 |
| Total error | 3.623 | 0.5176 | 11.655 | 1.665 | | | | |
| Lack of fit | 1.564 | 0.5212 | 1.01 | 0.475 | 7.076 | 2.359 | 2.06 | 0.248 |
| Pure error | 2.059 | 0.5149 | 4.579 | 1.145 | | | | |

dence level since the P-values were less than 0.05.

The F-test for lack of fit describes the variation of the data around the fitted model. If the model does not fit the data well, this will be significant. The large value for lack of fit (>0.05) shows that the F-statistics was insignificant, implying significant model correlation between the variables and process response [20]. The P-value of 0.478 for lack of fit for the turbidity removal and 0.302 for COD removal using $PFPD_1$ was greater than 0.05, indicating that the lack of fit was not significant. A high $R^2$ value, close to 1, is desirable and a reasonable agreement with adjusted $R^2$ is necessary [20]. A high $R^2$ coefficient ensures a satisfactory adjustment of the quadratic model to the experimental data. The $R^2$ value of 92.57% indicates that the turbidity removal model could not explain 7.43% of the total variations, while the $R^2$ value of 91.69% indicates that the COD removal model could not explain 8.31% of the total variations. In both instances, the $R^2$ value was close to the adjusted $R^2$ value.

The quadratic regression models for turbidity and COD removal efficiency using $PFPD_2$ are statistically significant at the 5% confidence level since the P-values are less than 0.05 (Table 3). The P-values of 0.475 and 0.248 for lack of fit for turbidity and COD removal are greater than 0.05, illustrating that the lack of fit is not significant. This implies that the models adequately describe the data. The $R^2$ value of 93.60% for turbidity removal indicates that the model could not explain 6.40% of the total variations, while the $R^2$ value of 96.45% for COD removal indicates that the model could not explain 3.55% of the total variations.

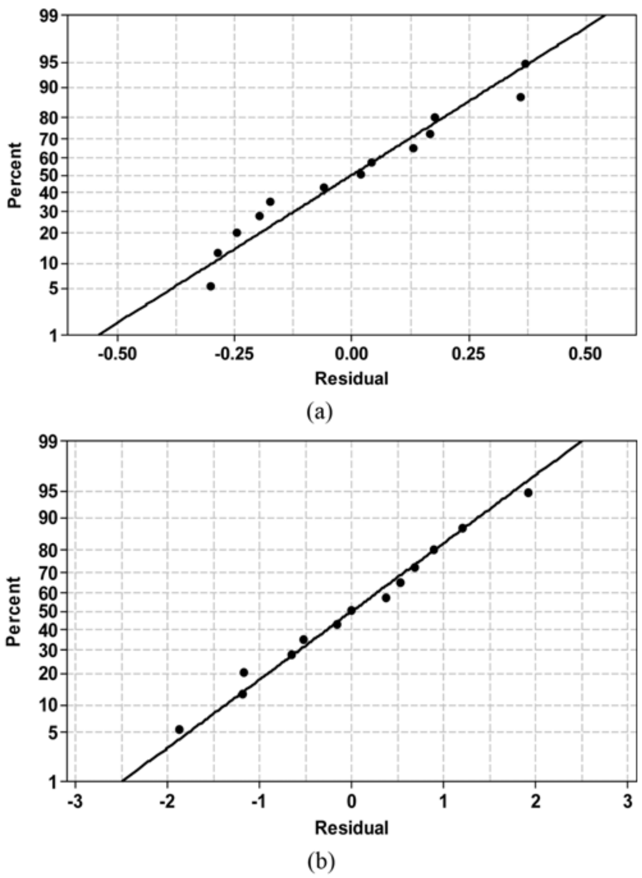


**Fig. 3. Normal probability plots for (a) turbidity and (b) COD removal efficiency using $PFPD_1$.**

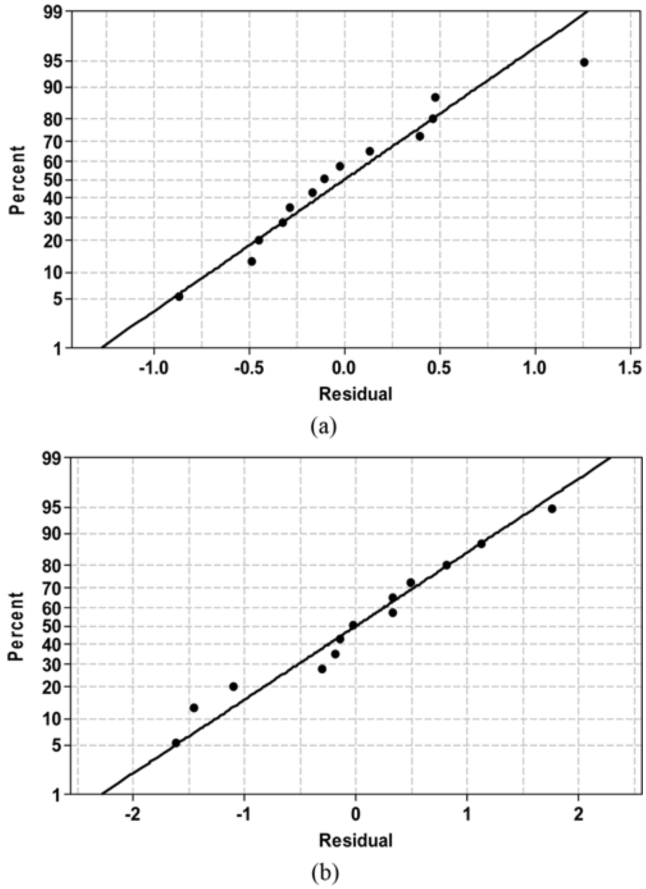


**Fig. 4. Normal probability for (a) turbidity and (b) COD removal efficiency using $PFPD_2$.**

Figs. 3 and 4 show the normal probability plot, in which the data were plotted against a theoretical normal distribution. For such plot, a departure from a straight line would indicate a departure from a normal distribution. The normal probability plots were used to check the normality distribution of the residuals. As shown in Figs. 3 and 4, it is reasonable that the assumption of normality was satisfied for the data. In addition, Figs. 5 and 6 show the predicted versus actual value plot of turbidity and COD removal. The predicted versus actual values plot was used to judge the model adequacy. The second-order regression model obtained for the operating variables of turbidity and COD removal was satisfied as the predicted versus actual value plot approximate a straight line as shown in Figs. 5 and 6.

**4. Optimization Analysis**

Figs. 7 and 8 show the plot of turbidity removal vs. COD removal data from the coagulation test. As shown, no clear correlation between these two responses is noted. Therefore, the removal mechanisms of turbidity and COD were different and the optimum conditions for the removal of each would also be different. Previous studies also reported that optimum conditions for turbidity removal are not always the same as those for NOM removal [5,6].

Table 4 gives an insight into the linear, quadratic and interaction effects of the parameters. The analysis was done by means of F- and T-tests. The T-test was used to determine the significance of the regression coefficients of the parameters, while the P-value was used as a tool to check the significance of each factor and interac-

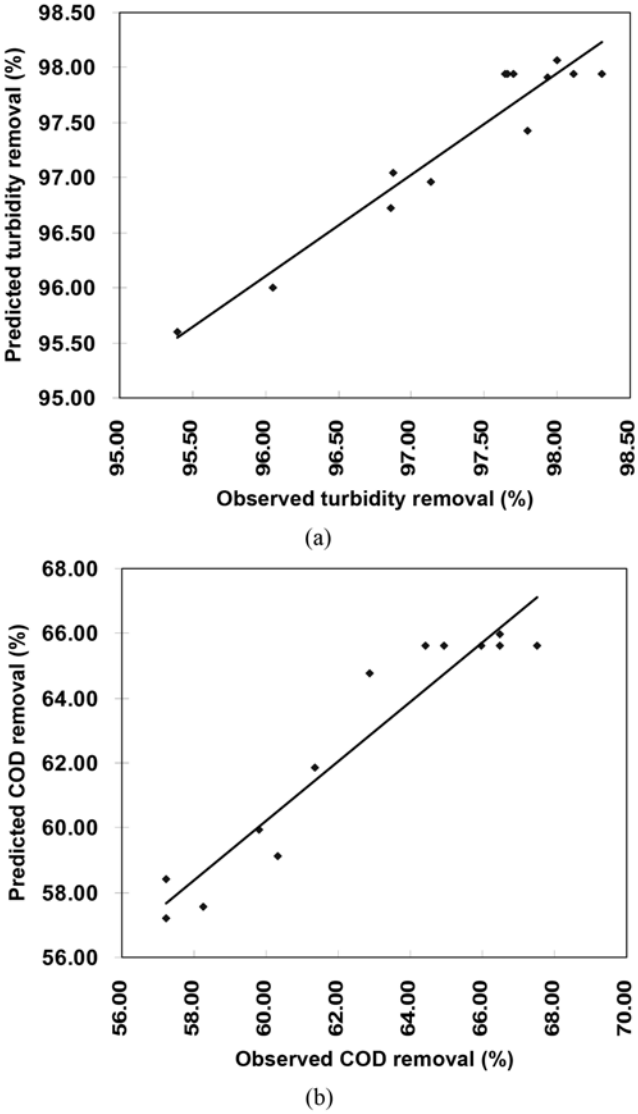


**Fig. 5. Predicted vs. observed (a) turbidity and (b) COD removal efficiency using $PFPD_1$.**

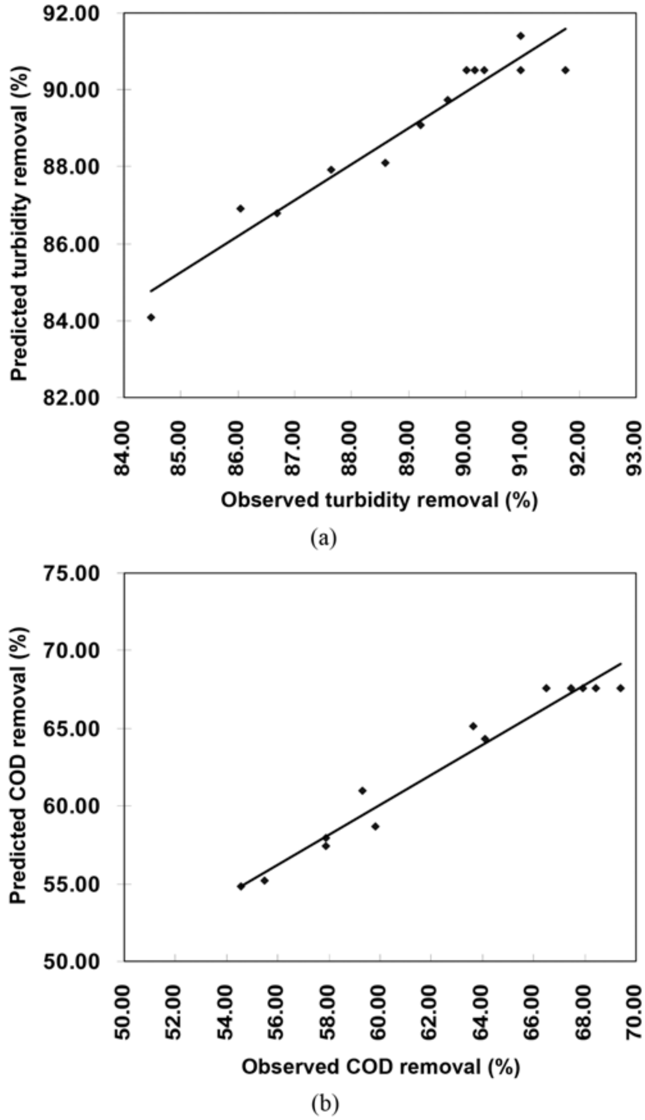


**Fig. 6. Predicted vs. observed (a) turbidity and (b) COD removal efficiency using $PFPD_2$.**

tion between factors. In general, the larger the magnitude of T and smaller the value of P, the more significant is the corresponding coefficient term [5,6]. Table 4 shows that the variable with the largest effect on turbidity removal using $PFPD_1$ was coagulation pH (quadratic) with a P-value of 0.002. The constant term, linear and quadratic effect of coagulant dosage (in the investigated range) could be considered to have no effect on the turbidity removal using $PFPD_1$, with P-values of 0.344, 0.145 and 0.111, respectively. However, for COD removal using $PFPD_1$, Table 4 shows that all the variables are highly significant with P-values less than 0.05. For turbidity removal using $PFPD_2$ all variables are highly significant except the coagulant dosage-coagulation pH (interaction) with a P-value of 0.054. In addition, for COD removal using $PFPD_2$ all variables are highly significant except the coagulant dosage (linear) with a P-value of 0.296.

Figs. 9 and 10 show the response surface plots for turbidity and COD removal. The response surface is the graphical representation of the regression equation used to visualize the relationship between

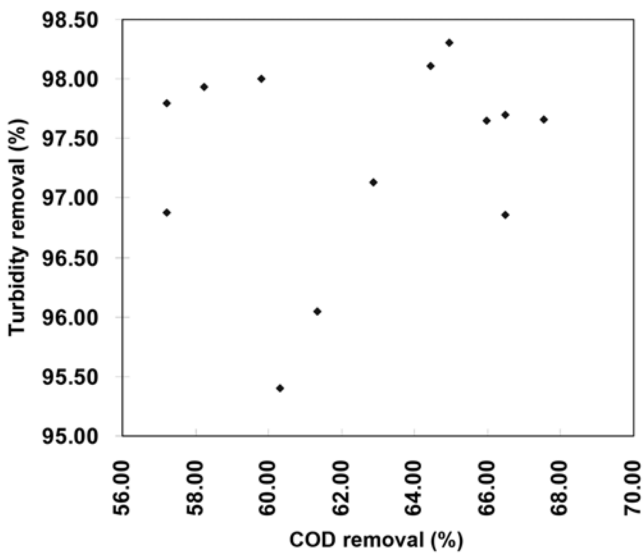


**Fig. 7. Plot of turbidity removal vs. COD removal using $PFPD_1$.**

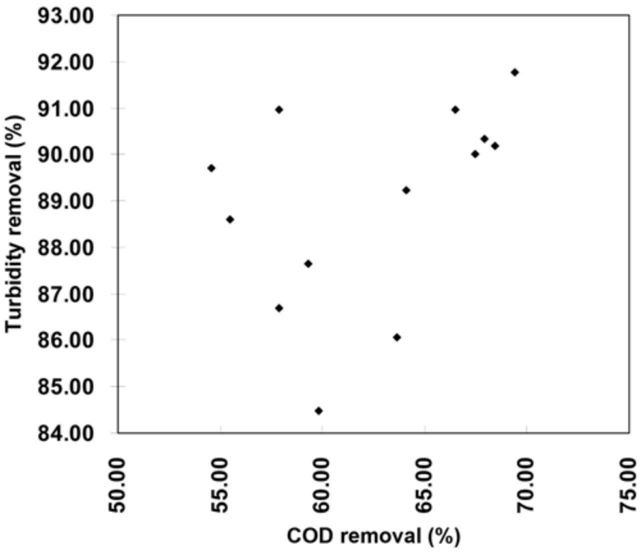


**Fig. 8. Plot of turbidity removal vs. COD removal using $PFPD_2$.**

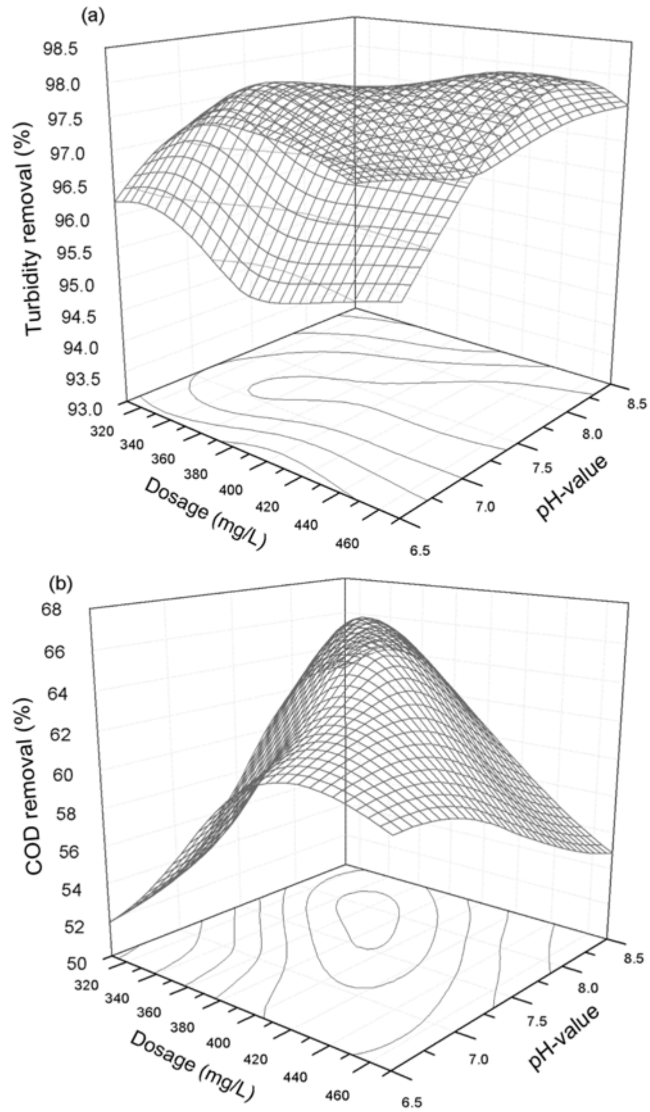


**Fig. 9. Response surface plots for (a) turbidity and (b) COD removal efficiency using $PFPD_1$.**

the response and experimental levels of each factor [5]. The convex shape of the response surface plots (Figs. 9 and 10) indicates that the best conditions for turbidity and COD removal are within the design area.

A number of previous studies have shown that coagulation of NOM by hydrolyzing metal salts is generally described as a combination of charge neutralization, entrapment, adsorption and complexation with coagulant metal hydrolysis species into soluble particulate aggregates. Wei et al. [21] indicated premixing PFC and PDADMAC before dosing, they competitively react with colloids and particles nearly at the same time. Because of the competition, only a few points of the PDADMAC chain were attached to the particles surface, while the bulk of the PDADMAC chain projected into the surrounding solution to adherence with particles much like a bridging mechanism [21]. Therefore, at lower coagulant dosages, the amount of polymer to form adequate bridging links between particles is insufficient, while with excess polymer, there is

**Table 4. Estimated regression coefficients and corresponding T- and P-values**

| | Turbidity removal | | | | COD removal | | | |
|---|---|---|---|---|---|---|---|---|
| | Coefficient | Standard error | T-value | P-value | Coefficient | Standard error | T-value | P-value |
| $PFPD_1$ | | | | | | | | |
| Constant | 28.5217 | 28.1133 | 1.015 | 0.344 | −880.969 | 129.450 | −6.805 | 0.000 |
| Dosage | −0.1071 | 0.0652 | −1.642 | 0.145 | 2.163 | 0.300 | 7.204 | 0.000 |
| pH | 23.5929 | 4.8527 | 4.862 | 0.002 | 138.470 | 22.345 | 6.197 | 0.000 |
| Dosage x Dosage | −0.0001 | 0.0000 | −1.823 | 0.111 | −0.001 | 0.000 | −6.989 | 0.000 |
| pH x pH | −2.1457 | 0.2552 | −8.408 | 0.000 | −5.119 | 1.175 | −4.357 | 0.003 |
| Dosage x pH | 0.0226 | 0.0076 | 2.954 | 0.021 | −0.155 | 0.035 | −4.399 | 0.003 |
| $PFPD_2$ | | | | | | | | |
| Constant | −297.073 | 66.2301 | −4.485 | 0.003 | −441.489 | 118.786 | −3.717 | 0.007 |
| Dosage | 0.786 | 0.1536 | 5.361 | 0.001 | 0.311 | 0.275 | 1.130 | 0.296 |
| pH | 61.284 | 11.4321 | 5.361 | 0.001 | 119.698 | 20.504 | 5.838 | 0.001 |
| Dosage x Dosage | −0.001 | 0.0001 | −5.993 | 0.001 | −0.002 | 0.000 | −10.061 | 0.000 |
| pH x pH | −3.048 | 0.6012 | −5.070 | 0.001 | −11.327 | 1.078 | −10.505 | 0.000 |
| Dosage x pH | −0.042 | 0.0180 | −2.313 | 0.054 | 0.132 | 0.032 | 4.079 | 0.005 |

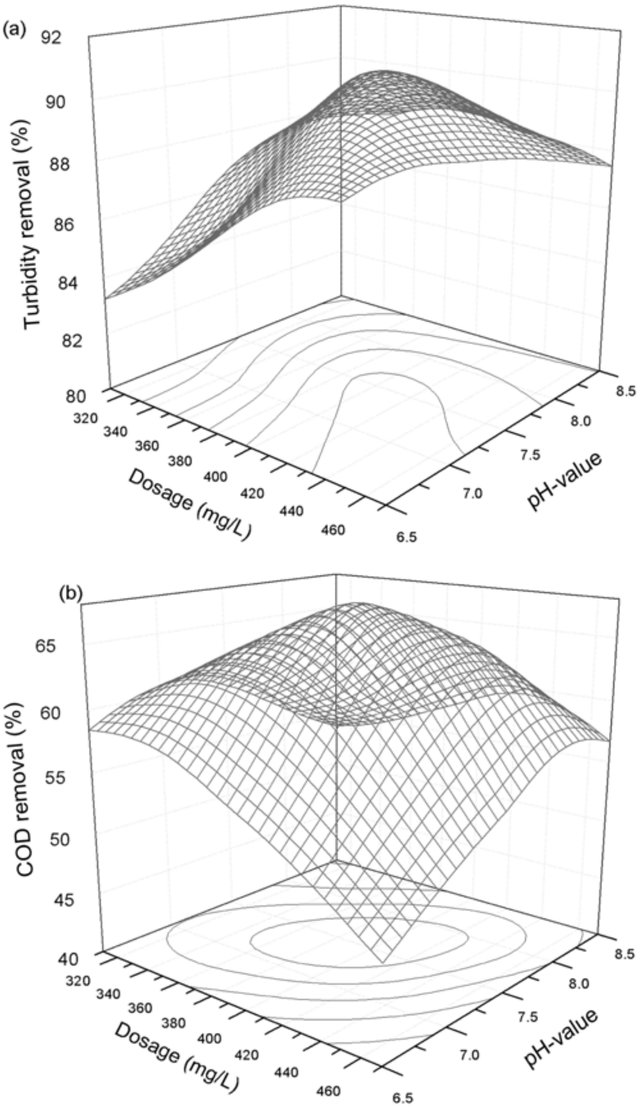


**Fig. 10. Response surface plots for (a) turbidity and (b) COD removal efficiency using PFPD$_2$.**

no longer enough bare particle surface available for attachment of segments resulting in particle destabilization. As a result, there should be an optimum polymer dosage for coagulation-flocculation [15]. Fig. 9 shows that the maximum turbidity removal efficiency using PFPD$_1$ is in the region where the coagulant dosage ranges from 420 to 450 mg/L, whereas for COD removal, the maximum is in the region where the coagulant dosage ranges from 330 to 380 mg/L. As can be seen from Fig. 10, the maximum turbidity removal efficiency using PFPD$_2$ is in the region where the coagulant dosage ranges from 390 to 470 mg/L, whereas for COD removal, the maximum is in the region where the coagulant dosage ranges from 360 to 420 mg/L.

Zhu et al. [15] attributed the increase in the turbidity and COD removal efficiency at pH 5-8 to hydroxyl ions reacting with Fe$_a$ species to produce more ferrite polymers, thus improving the bridging flocculation. At the same time, the colloid surface charge decreases due to the charge neutralization mechanism, enhancing the destabilization of the colloidal particles in water. However, at high alkaline environment, the coagulant will be susceptible to hydrolysis, inhibiting the bridging flocculation. Therefore, there should be an optimum coagulation pH to maximize the performance of coagulation [15]. Fig. 9 shows that the maximum turbidity removal efficiency using PFPD$_1$ is in the region where the coagulation pH ranges from 7.6-8.2, whereas for COD removal, the maximum is in the region where the coagulation pH ranges from 7.7-8.3. Furthermore, Fig. 10 illustrates the maximum turbidity removal efficiency using PFPD$_2$ is in the region where the coagulation pH ranges from 6.5-7.6, whereas for COD removal, the maximum is in the region where the coagulation pH ranges from 7.2-7.9. In general, the response surface plots clearly indicate that the maximum removal efficiencies are located inside the design boundary.

Using the Minitab-16 response optimizer, the model (Eq. (2)) predicted the turbidity removal efficiency of 98.1% could be achieved at a coagulant dosage of 430 mg/L and coagulation pH of 7.96 using PFPD$_1$. Eq. (3) predicts a removal efficiency of 66.2% at a coagulant dosage of 384 mg/L and coagulation pH of 8.13 for COD removal. The turbidity and COD removal are two individual responses, and their optimization was achieved under different optimal conditions. Thus, the optimum turbidity removal might impact COD removal and vice versa. Therefore, a compromise between the optimum conditions for the two responses is desirable [5]. The response optimizer was used in optimizing Eqs. (2) and (3) simultaneously; the optimum condition was coagulant dosage of 384 mg/L and coagulation pH of 7.75. Under optimum conditions, the predicted turbidity and COD removal efficiencies were 97.8% and 65.8%. However, the results of the confirmation experiments show turbidity and COD removal efficiencies at optimum conditions of 96.86% and 66.39%, indicating that the obtained results were close to the model estimates. This implies that the RSM approach was appropriate for optimizing the conditions of the coagulation-flocculation process using PFPD$_1$.

Furthermore, using the response optimizer, the model (Eq. (4)) predicted the turbidity removal efficiency of 90.5% could be achieved at a coagulant dosage of 390 mg/L and coagulation pH of 7.28 using PFPD$_2$. Eq. (5) predicts a removal efficiency of 67.6% at a coagulant dosage of 390 mg/L and coagulation pH of 7.49 for COD removal. Optimizing Eqs. (4) and (5) simultaneously, the optimum condition was coagulant dosage of 390 mg/L and coagulation pH of 7.48. Under optimum conditions, the predicted turbidity and COD removal efficiencies were 90.5% and 67.6%. The measured turbidity and COD removal efficiencies at optimum conditions were 90.31% and 67.92%, which shows that the obtained results were close to the model estimates. This implies that the RSM approach was appropriate for optimizing the conditions of the coagulation-flocculation process using PFPD$_2$.

## CONCLUSIONS

Optimization of the coagulation-flocculation process with respect to turbidity and COD removal efficiency using PFPD$_1$ and PFPD$_2$ has been investigated. RSM using the CCD was applied to determine the optimum operating conditions for maximum removal of turbidity and COD. Using PFPD$_1$, the results indicate that the coagulant dosage (in the range investigated) could be considered to have no effect on the turbidity removal efficiency, while the interaction between coagulant dosage and coagulation pH was less significant for turbidity removal using $PFPD_2$. At optimum conditions, 65.8% COD removal was achieved using $PFPD_1$, whereas removalusing $PFPD_2$ was 67.6%. In contrast, the turbidity removal efficiency at optimum conditions was 97.8% and 90.5% for $PFPD_1$ and $PFPD_2$, respectively. Therefore, this study reveals that despite an increase in the PDADMAC content of the composite coagulant, the decrease in the turbidity removal efficiency was high while the increase in the COD removal efficiency was minimal. The results of the confirmation experiment were found to be in good agreement with the values predicted by the model. This demonstrates that to obtain a maximum amount of information in a short period of time, with the least number of experiments, RSM and CCD can be successfully applied for modeling and optimizing the coagulation-flocculation process.

## ACKNOWLEDGEMENTS

The authors are grateful for the financial support provided by the National Natural Science Foundation of China (Project No. NSFC, 51078366, 21177164), the Cultivation Fund of the Key Scientific and Technical Innovation Project, Ministry of Education of China (No. 708071).

## REFERENCES

1. J. Q. Jiang and N. J. D. Graham, *Water Res*., **32**, 930 (1998).
2. A. I. Zouboulis and P. A. Moussas, *Desalination*, **224**, 307 (2008).
3. H. Z. Zhao, Z. K. Luan, B. Y. Gao and Q. Y. Yue, *J. Appl. Polym. Sci.*, **84**, 335 (2002).
4. Y. Wang, B. Y. Gao, Q. Y. Yue, J. C. Wei and Q. Li, *Chem. Eng. J*., **142**, 175 (2008).
5. T. K. Trinh and L. S. Kang, *Environ. Eng. Res*., **15**(2), 63 (2010).
6. T. K. Trinh and L. S. Kang, *Chem. Eng. Res. Des.*, **89**, 1126 (2011).
7. D. C. Montgomery, *Design and analysis of experiments*, 5th Ed., John Wiley & Sons, New York (2001).
8. C. P. Xu, S. W. Kim, H. J. Hwang, J. W. Choi and J. W. Yun, *Process Biochem.*, **38**, 1025 (2003).
9. A. L. Ahmad, S. S. Wong, T. T. Teng and A. Zuhairi, *J. Hazard. Mater.*, **145**, 162 (2007).
10. J. P. Wang, Y. Z. Chen, X. W. Ge and H. Q. Yu, *Colloid Surface A*, **302**, 204 (2007).
11. F. M. Omar, N. N. N. A. Rahman and A. Ahmad, *Water, Air, Soil Pollut.*, **195**, 345 (2008).
12. O. S. Amuda and I. A. Amoo, *J. Hazard. Mater.*, **141**, 778 (2007).
13. S. Chowdhury, S. Chakraborty and P. D. Saha, *Environ. Sci. Pollut. Res.*, DOI: 10.1007/s11356-012-0989-7 (2012).
14. P. D. Saha, S. Chowdhury and S. Das, *Arch. Environ. Sci.*, **6**, 57 (2012).
15. G. Zhu, H. L. Zheng, Z. Zhang, T. Tshukudu, P. Zhang and X. Xiang, *Chem. Eng. J*., **178**, 50 (2011).
16. B. Y. Gao, Y. Wang, Q. Y. Yue, J. C. Wei and Q. Li, *Sep. Purif. Technol.*, **62**, 544 (2008).
17. Y. Zeng and J. Park, *Colloid Surface A*, **334**, 147 (2009).
18. H. L. Zheng, G. Zhu, S. Jiang, T. Tshukudu, X. Xiang, P. Zhang and Q. He, *Desalination*, **269**, 148 (2011).
19. V. Jaikumar and V. Ramamurthi, *J. Modern Appl. Sci.*, **3**(4), 71 (2009).
20. S. Ghafari, H. A. Aziz, M. H. Isa and A. A Zinatizadeh, *J. Hazard. Mater.*, **163**, 650 (2009).
21. J. C. Wei, B. Y. Gao, Q. Y. Yue, Y. Wang and L. Lu, *J. Hazard. Mater.*, **165**, 789 (2009).